Exotic vortex wakes—point vortex solutions

H. Aref[a,*], M.A. Stremler[b], F.L. Ponta[c]

[a]*Department of Engineering Science and Mechanics, Virginia Polytechnic Institute and State University, Blacksburg, VA, USA*
[b]*Department of Mechanical Engineering, Vanderbilt University, Nashville, TN, USA*
[c]*College of Engineering, University of Buenos Aires, Argentina*

Abstract

Von Kármán was the first to present a quantitative model of the "vortex street" wake as a double row of point vortices, to determine which configurations propagate in the direction of the rows, and to consider the linear stability theory for such states. In the early literature one works with infinite rows of vortices. The vortex street is assumed to continue to infinity both upstream and downstream. Another analytical approach is to use periodic boundary conditions in the direction of the wake. This representation was used by Domm in his analysis of the instability of the Kármán vortex street. Birkhoff and Fisher in 1959 were the first to treat vortices in a periodic strip as a dynamical system in its own right. We have used the periodic system to address problems of vortex wake patterns, in particular vortex wakes that are more complicated than the traditional two-vortices-per-strip configurations. We use the term "exotic" for such wakes. We submit that this approach can yield a number of insights, including results of direct relevance to experiments, in the same sense that von Kármán's analysis has been helpful to the understanding of the regular vortex street wake, and we present the results obtained to date following this program.
© 2006 Elsevier Ltd. All rights reserved.

1. Introduction

The driving theme of the research program described in this paper is to use point vortex models as a guide to the understanding of more complex—we use the term "exotic"—vortex wake patterns in the same way they have guided our understanding of the "simple" Kármán vortex street for close to a century.

Vortex wake modelling using point vortices goes back to the seminal 1911–1912 papers of von Kármán, as elaborated in the well-known treatise of Lamb (1932). Von Kármán addressed the structure and linearized stability of vortex street wakes and, with Rubach, found the form of the drag law for the force exerted on a bluff body by a vortex street wake.

Both von Kármán and Lamb use infinite rows of point vortices in their analysis. We prefer to look at segments of the vortex wake and assume it to be periodically continued indefinitely to both sides. In this way, as argued already by Aref (1983), the analysis addresses modes of ever longer wavelength, and ever increasing complexity, in a systematic fashion. The basic equations for point vortices in a periodic strip appear to have been first given by Friedmann and Poloubarinova (1928). Rosenhead (1929) used these equations in his early discussion and numerical simulations of

---

*Corresponding author. Tel.: +1 540 231 5626.
E-mail address: haref@vt.edu (H. Aref).

vortex sheet roll-up and wake transitions. Two vortices per strip width suffice for a full discussion of vortex street structure and translational velocity. Domm (1956) showed that four vortices per strip, two of either sign, suffice for a comprehensive study of the stability of a vortex street. This includes a demonstration of the instability of a point vortex street with the von Kármán ratio between width and intra-row spacing to perturbations of higher order. These results had been found previously by Kochin (1939) using infinite vortex rows.

Birkhoff and Fisher (1959) appear to be the first to discuss vortices in a periodic strip as a "standalone" dynamical system. They show that the system is Hamiltonian and identify its general integrals of motion. Aref and Stremler (1996) have solved the problem of three vortices with sum of circulations zero in a periodic strip. Much of our analysis of "exotic wakes" is based on the results of this work.

In Section 2 we first review briefly how the main results on the structure and translational velocity for the Kármán street can be derived from a two-vortices-in-a-periodic-strip analysis, and we cite the results of Domm (1956) without much elaboration. In Section 3 we move on to three vortices in a periodic strip. We first review the solution for three vortices of net circulation zero on the infinite plane following Rott (1989) and Aref (1989). This work sets the stage for understanding the extension to the periodic strip by Aref and Stremler (1996).

We are now ready to address the "exotic wake" problem in Section 4, at least insofar as the case of three vortices per shedding cycle is concerned. It immediately appears that known experimental and numerically computed patterns fall short in representing the richness revealed in the solution of three-vortices-per-strip dynamics. We give an account of work by Stremler (2003) to find vortex street patterns with three vortices per period that translate uniformly in the streamwise direction. Apparently, none of these patterns have been seen experimentally.

In Section 5 we reflect on the results that we have and draw preliminary conclusions. We mention a class of solutions of stationary wake patterns that arise as a corollary of the three-vortex-in-a-strip investigation and that, potentially, define an entirely new class of wakes with vanishing impulse.

2. Point vortices in a periodic strip

The equations of motion for a system of N point vortices, located at positions $z_1, \ldots, z_N$ and with circulations $\Gamma_1, \ldots, \Gamma_N$, respectively, on the infinite plane—here represented as the complex plane—are

$$\overline{\frac{\mathrm{d}z_\alpha}{\mathrm{d}t}} = \frac{1}{2\pi\mathrm{i}} \sum_{\beta=1}^{N}{}' \frac{\Gamma_\beta}{z_\alpha - z_\beta}. \tag{1}$$

In (1) the prime on the sum on the right-hand side indicates omission of the singular term $\beta = \alpha$, and the overline on the left-hand side indicates complex conjugation.

We impose periodic boundary conditions, so that each vortex in "the basic strip" has periodic images extending to infinity on the right and on the left of the basic strip. That is, each z_α, $\alpha = 1, \ldots, N$, now represents a row of vortices located at $z_\alpha \pm nL$, where L is the strip width and $n = 0, 1, 2, \ldots$ runs through the integers. If this representation is substituted into Eqs. (1), and if the conditionally convergent sum over image vortices is performed by summing images corresponding to $\pm n$ pairwise, we obtain the following system of dynamical equations:

$$\overline{\frac{\mathrm{d}z_\alpha}{\mathrm{d}t}} = \frac{1}{2L\mathrm{i}} \sum_{\beta=1}^{N}{}' \Gamma_\beta \cot\left[\frac{\pi}{L}(z_\alpha - z_\beta)\right]. \tag{2}$$

These are the equations derived by Friedmann and Poloubarinova (1928). They were used by Rosenhead (1929) in his analysis and early simulations of vortex sheet roll-up and vortex street dynamics (see Rosenhead, 1931).

Equations (2) share many properties of the equations of motion on the infinite plane. The periodic strip system may be cast in Hamiltonian form. Two of the integrals familiar from the infinite plane case, the components of the linear impulse, X and Y,

$$X + \mathrm{i}Y = \sum_{\alpha=1}^{N} \Gamma_\alpha z_\alpha, \tag{3}$$

remain integrals for the periodic strip system, as seems first to have been emphasized by Birkhoff and Fisher (1959).

A simple consequence of Eqs. (1) is worth noting. Assume a configuration of the base vortices $\alpha = 1, 2, \ldots, N$ is given for which the configuration translates like a rigid body with complex velocity $U + \mathrm{i}V$, where U and V are the two real components of the translation velocity. The left-hand side in each of Eqs. (1) is then $U - \mathrm{i}V$. Multiply the equation for vortex α by Γ_α and sum over α from 1 to N. By the antisymmetry of the summand on the right-hand side in the two

indices α and β we obtain

$$S(U - iV) = 0,$$ (4)

where S is the sum of the circulations of the N base vortices. Thus, we have the result that a vortex configuration representing a relative equilibrium can only have a finite translation velocity if the sum of the circulations of the N base vortices vanishes.

The classical Kármán vortex street model may be captured by the system $N = 2$ with $\Gamma_1 = -\Gamma_2 = \Gamma$. The equations of motion in this case are

$$\frac{\overline{dz_1}}{dt} = -\frac{\Gamma}{2Li}\cot\left[\frac{\pi}{L}(z_1 - z_2)\right], \quad \frac{\overline{dz_2}}{dt} = \frac{\Gamma}{2Li}\cot\left[\frac{\pi}{L}(z_2 - z_1)\right].$$ (5)

It follows directly from these equations, or from (3), that $z_1 - z_2$ is a constant of the motion. Let us set $z_1 - z_2 = a + ib$. Then the two vortex rows translate with velocity $U + iV$ given by

$$U - iV = -\frac{\Gamma}{2Li}\cot\left[\frac{\pi}{L}(a + ib)\right].$$ (6)

If this translation is to be along the x-axis, $\cot[\pi(a + ib)/L]$ must be pure imaginary, which implies $\sin(2\pi a/L) = 0$ or that a either vanishes or equals $L/2$. In order for a vortex street to translate along the rows, it must either be symmetrical or staggered. Substituting $a = 0$ and $L/2$, respectively, in (6) gives the well-known formulae for the translation velocity of a symmetrical and a staggered vortex street.

The stability problem for vortex streets was addressed by Domm (1956) using the problem of four vortices in a strip, all with strengths of the same magnitude, two of either sign. This analysis captures a surprising amount of the full problem. (i) It shows that unless the street dimensions a and b satisfy

$$\sinh\frac{\pi b}{h} = \sin\frac{\pi a}{h},$$ (7)

where h is the spacing between vortices in either row.[1] The condition (7) which pertains to all vortex streets, including those translating at an angle to the x-axis, is due to Dolaptschiew (1938) and Maue (1940). It shows that the symmetric vortex street, $a = 0$, can never be linearly stable, but the staggered vortex street, $a = h/2$, may be stable if $\sinh(\pi b/h) = 1$. This special case of (7) is the famous condition found by von Kármán. (ii) Even when (7) is satisfied, Domm's analysis shows that the vortex street is unstable to second order perturbations. Thus, none of the point vortex streets are stable—not even the ones satisfying the criterion (7)—and the prevalence of such patterns in laboratory and numerical experiments must be due to other stabilizing effects or is simply the reflection of a particularly long-lived transient.

3. Three point vortices with zero net circulation in a periodic strip

We now turn to the dynamics of three vortices in a strip. Using the theory of Hamiltonian systems, in particular the construct of Poisson brackets and Liouville's theorem, one can show that the periodic three-vortex system is integrable if the sum of the three circulations is zero. This problem, then, seems "made to order" for a discussion of shedding patterns from a bluff body in which three vortices are shed in each cycle, since one usually assumes the vanishing of the sum of the circulations of the vortices shed in a shedding cycle.

The full solution of the integrable three-vortices-in-a-strip problem is quite rich. To set the stage for an overview of the results it is useful to first review the simpler problem of three vortices with net circulation zero on the infinite plane following Rott (1989) and Aref (1989).

3.1. Three point vortices with zero net circulation on the infinite plane

At issue is the solution of the following equations where $\Gamma_1 + \Gamma_2 + \Gamma_3 = 0$:

$$\frac{\overline{dz_1}}{dt} = \frac{1}{2\pi i}\left(\frac{\Gamma_2}{z_1 - z_2} + \frac{\Gamma_3}{z_1 - z_3}\right), \quad \frac{\overline{dz_2}}{dt} = \frac{1}{2\pi i}\left(\frac{\Gamma_1}{z_2 - z_1} + \frac{\Gamma_3}{z_2 - z_3}\right), \quad \frac{\overline{dz_3}}{dt} = \frac{1}{2\pi i}\left(\frac{\Gamma_1}{z_3 - z_1} + \frac{\Gamma_2}{z_3 - z_2}\right).$$ (8)

---

[1] We need a different symbol for this entity since, while $h = L$ for two vortices per strip, $h = L/2$ for a vortex street configuration viewed as a state of four vortices per strip.
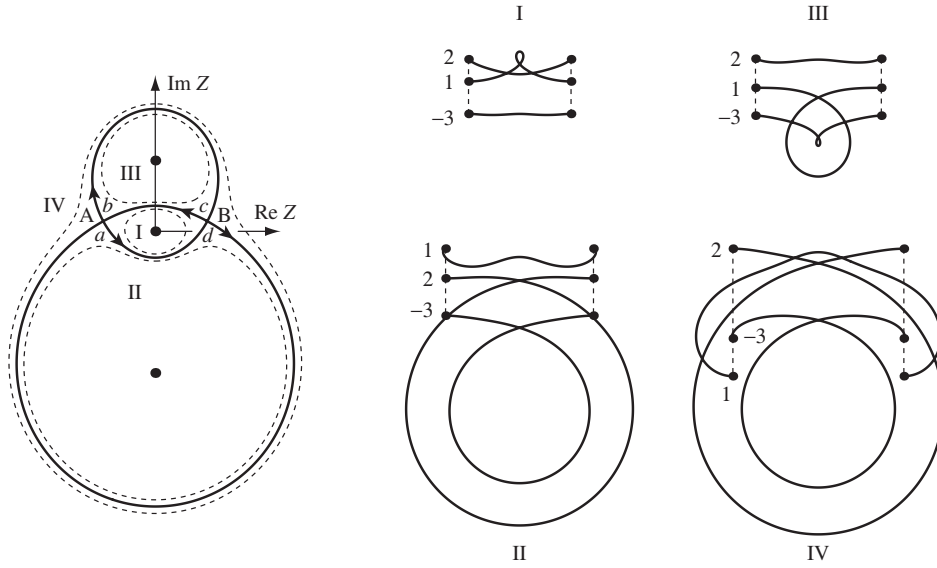
Fig. 1. Phase plane diagram and physical plane trajectories for the three-vortex problem on the infinite plane with $(\Gamma_1, \Gamma_2, \Gamma_3) = (2, 1, -3)$. At left, solid lines are separatrices delimiting the four domains of motion I–IV. Dashed lines correspond to real space motions shown at right labelled by the domain's Roman numeral. Values of X and Y, Eq. (3), are 0 and 1, respectively. At right, vortices are labelled by their strengths. Motions are shown for one period of the relative motion.

If we set $Z = z_1 - z_2$, we notice that all the vortex separations may be expressed in terms of Z and entities that are constant throughout the motion. Thus, from

$$\Gamma_1 z_1 + \Gamma_2 z_2 + \Gamma_3 z_3 = X + iY \tag{9}$$

and the vanishing sum of the vortex strengths we get

$$z_2 - z_3 = \frac{\Gamma_1 Z - \Xi}{\Gamma_3}, \quad z_3 - z_1 = \frac{\Gamma_2 Z + \Xi}{\Gamma_3} \quad \text{where} \, \Xi = X + iY. \tag{10}$$

Subtracting the second Eq. (8) from the first then gives an equation of motion for Z:

$$\frac{\overline{dZ}}{dt} = -\frac{\Gamma_3^2}{2\pi i}\left(\frac{\Gamma_3^{-1}}{Z} + \frac{\Gamma_2^{-1}}{Z + \Xi/\Gamma_2} + \frac{\Gamma_1^{-1}}{Z - \Xi/\Gamma_1}\right). \tag{11}$$

This equation may be interpreted as the equation of motion for a particle at Z advected by three vortices of relative strengths $\Gamma_3^{-1} : \Gamma_2^{-1} : \Gamma_1^{-1}$ and located, respectively, at the origin, at $-\Xi/\Gamma_2$ and at Ξ/Γ_1. Note that while the three original strengths, Γ_1, Γ_2 and Γ_3, sum to zero, the sum of the strengths of the three advecting vortices in Eq. (11), $\Gamma_3^{-1} + \Gamma_2^{-1} + \Gamma_1^{-1}$, is nonzero. We have also taken advantage of the possibility in this problem of rotating the coordinates such that Ξ is pure imaginary.[2] This choice allows us to bring out the correspondence with the periodic strip case more clearly.

The steady advection problem for Z is easily solved by constructing the streamfunction of the flow due to the three vortices. An example for the convenient prototypical case $(\Gamma_1, \Gamma_2, \Gamma_3) = (2, 1, -3)$ is shown in Fig. 1. We refer to the flow plane in which the three original vortices move about as the 'physical plane'. The Z-plane we call the 'phase plane'. To each motion in the Z-plane there corresponds a relative motion of the three vortices in the physical plane. Since the Z-motions are periodic, we conclude that the relative motion of the three vortices is periodic. That is, the vortex configuration in the physical plane—in Fig. 1 always chosen as initially collinear—returns to the same shape and size after a finite time. However, the final configuration will generally be displaced relative to its original position. This displacement is an example of what Newton (2001) calls Berry's phase.

The phase plane diagram in Fig. 1 is divided into four domains designated by Roman numerals I–IV. Each domain corresponds to a range of motions that are qualitatively similar. Thus, motions in domain I, where the Z-point orbits

---

[2] $\Xi = 0$ corresponds to the three vortices being on a line in a configuration that rotates like a rigid body.

the origin, correspond to three-vortex motion where the vortices of strength 1 and 2 are always close and move as a unit with vortex 3 at some distance. In domain II (III) the vortices with strengths 2 (1) and −3 form a bound pair that moves, more or less, as such a pair would move on the infinite plane while translating along with the other positive vortex at some distance. Domain IV is the most highly interactive regime of motion with no obvious pairing of vortices. Examples of vortex trajectories corresponding to the four domains are illustrated in the right-hand side of Fig. 1. All trajectory segments correspond to one period of the relative motion. The dashed lines in the phase plane correspond to the physical space motions shown.

The two saddle points, labelled A and B, in the phase plane of Fig. 1, correspond to equilateral triangle configurations. An equilateral triangle of point vortices of any strengths (whether they add to zero or not) moves without change of shape or size. When the sum of the circulations is zero, the triangle translates along the direction singled out by the impulse. Thus, the states A and B in Fig. 1 are translating equilateral vortex triangles. In Fig. 2 we show the streamline pattern around one of these two translating equilateral triangles.

The relative equilibria A and B are unstable to small perturbations. For a perturbation that maintains energy, the vortex configuration will evolve dynamically along one of the separatrices labelled a, b, c and d in Fig. 1. These correspond to motions in which the triangle changes its orientation from counter-clockwise to clockwise or vice versa. In Fig. 3 we show physical plane motions corresponding to the separatrices. The relative motion is, of course, not periodic in these cases, so Fig. 3 shows the motion for a time interval centered on the re-orientation "event".

The three advecting vortices in the phase plane of Fig. 1 actually form a stationary equilibrium. To see this note that Z coinciding with one of them corresponds to the superposition of two of the original vortices. But in this limit the three-vortex problem reduces to a two-vortex problem with opposite vortices. As we saw in Section 2 the solution to the
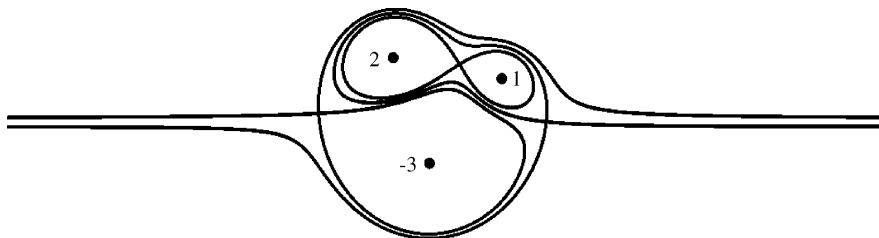

Fig. 2. Physical plane streamlines in the co-moving frame for the equilateral triangle relative equilibrium that corresponds to point A in Fig. 1. This configuration translates from left to right. Point B corresponds to a configuration that is the mirror image of this one in a line perpendicular to the direction of propagation.
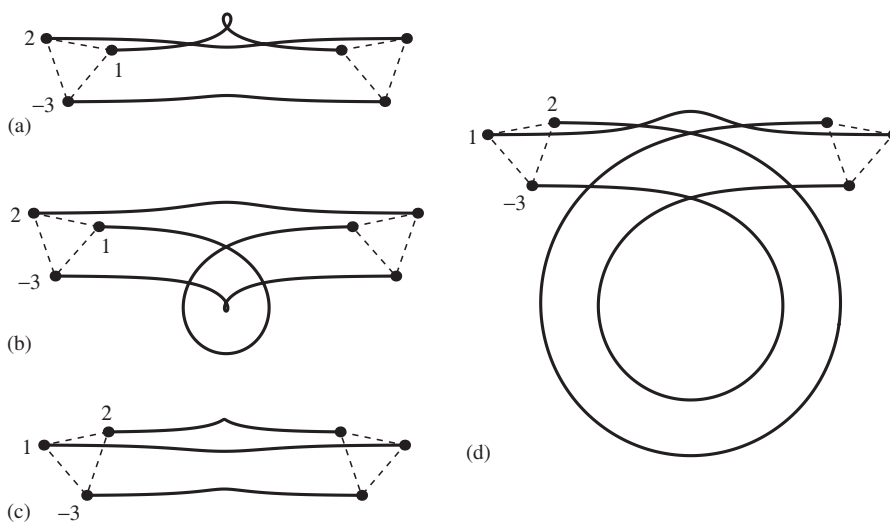

Fig. 3. Re-orientation of the equilateral triangle in the physical plane as the phase point passes from A to B (B to A), panels (a) and (b) (panels (c) and (d)) in Fig. 1. Labels correspond to labels of separatrices in Fig. 1.

two-vortex problem is uniform translation, i.e., Z is fixed. This means that the induced velocity at each of the advecting vortices in the phase plane of Fig. 1 must vanish.

3.2. Extension to the periodic strip

For three vortices in a periodic strip, the equations to be solved are

$$\frac{\overline{dz_1}}{dt} = -i[\Gamma_2 C(z_1 - z_2) + \Gamma_3 C(z_1 - z_3)], \tag{12}$$

$$\frac{\overline{dz_2}}{dt} = -i[\Gamma_1 C(z_2 - z_1) + \Gamma_3 C(z_2 - z_3)], \tag{13}$$

$$\frac{\overline{dz_3}}{dt} = -i[\Gamma_1 C(z_3 - z_1) + \Gamma_2 C(z_3 - z_2)], \tag{14}$$

where $\Gamma_1 + \Gamma_2 + \Gamma_3 = 0$ and $C(z) = \cot(\pi z/L)/2L$.

The extension of the analysis proceeds initially along the same lines as in the infinite plane case. The three intra-vortex separations can, once again, be expressed in terms of one of them, Z, and constant quantities, as in Eq. (10). The main difference arises when we subtract (13) from (12). We now get

$$\frac{\overline{dZ}}{dt} = i\Gamma_3 \left\{ C(Z) + C\left[\frac{\Xi}{\Gamma_3} + \left(\gamma - \frac{1}{2}\right)Z\right] - C\left[\frac{\Xi}{\Gamma_3} + \left(\gamma + \frac{1}{2}\right)Z\right] \right\}, \tag{15}$$

where $\gamma = \Gamma_2/\Gamma_3 + 1/2$.

We see that the three terms in (15) correspond to periodic strips of different widths. The term $C(Z)$ has the original period L. The other two terms have strip periods $L/(\gamma + 1/2) = L|\Gamma_3|/\Gamma_1$ and $L/(\gamma - 1/2) = L|\Gamma_3|/\Gamma_2$, respectively.

In Aref and Stremler (1996) it is shown that Eq. (15) can, nevertheless, be interpreted as an advection problem. The advecting vortices form three rows. In the first row the vortices all have strength Γ_3^{-1} and they are located at nL, where $n = 0, \pm 1, \pm 2, \ldots$. In the second row the vortices all have strength Γ_2^{-1} and their positions are given by $(-\Xi + n\Gamma_3 L)/\Gamma_2$, $n = 0, \pm 1, \pm 2, \ldots$. In the third row the vortices all have strength Γ_1^{-1} and their positions are $(\Xi + n\Gamma_3 L)/\Gamma_1$, where $n = 0, \pm 1, \pm 2, \ldots$. These vortex strengths and the location of the vortex with $n = 0$ will be familiar from the infinite plane problem. In this problem Ξ is, in general, a complex constant. Rotation of coordinates to make Ξ purely imaginary, as on the infinite plane, is no longer possible.

When γ is rational, the three vortex rows are commensurate and can all be captured in a wider strip. When γ is irrational, the advecting vortices do not have long-range spatial order along the x-axis. In this case, and in the analogous situation for doubly periodic vortex systems, we call such structures *vortex quasi-crystals*.

In Fig. 4 we show an example of the phase plane for three vortices in a periodic strip when $(\Gamma_1, \Gamma_2, \Gamma_3) = (2, 1, -3)$. This is a commensurate case and the entire phase plane diagram fits into a strip of width $3L$. We have shown two copies of this strip in order to clearly display the structure straddling the periodic boundary. This structure is similar to the phase plane diagram for the unbounded flow case. The value of Ξ has been determined numerically such that the relative equilibrium corresponding to point A will translate in the periodic direction, i.e., along the x-axis (see Section 4 for how this is done).

We have again labelled the various domains by Roman numerals, reserving I–IV for those domains that correspond to the infinite plane case in Fig. 1. There are now numerous additional domains. Some of these, e.g., VII, are quite thin and have many twists and turns across the entire periodic strip. The domains V and VI are, by contrast, quite large, extending off to positive and negative complex infinity, respectively. Domains such as V–VII, that exit and re-enter successive periodic strips allow motions in which $\Re(Z) = x_1 - x_2$ can increase linearly in time without bounds. Other domains, such as I–III and several unlabelled domains, imply bounded variation of $x_1 - x_2$ (and, thus, of any x-coordinate difference between vortices). Physical plane trajectories corresponding to the domains I–IV, that are similar to the domains seen in the infinite plane case, are shown in Fig. 5.

In Fig. 6 we show physical plane trajectories corresponding to domains V–VII. The trajectories in domains V and VI have the qualitative feature that a pair of vortices of opposite-signed circulations moves in one direction (to the right in V, to the left in VI), while the third vortex moves in the opposite direction. This qualitative feature is currently one of the few correspondences between this theory and existing data on vortex wakes with three vortices per shedding cycle. These trajectories also demonstrate that the periodicity of the relative configuration may involve the periodic images of the vortices. Thus, in Fig. 6(V) the three vortices start out on a line but after one period of the relative motion the new collinear configuration is made up of the original vortex with strength 2 and periodic images of the vortices with
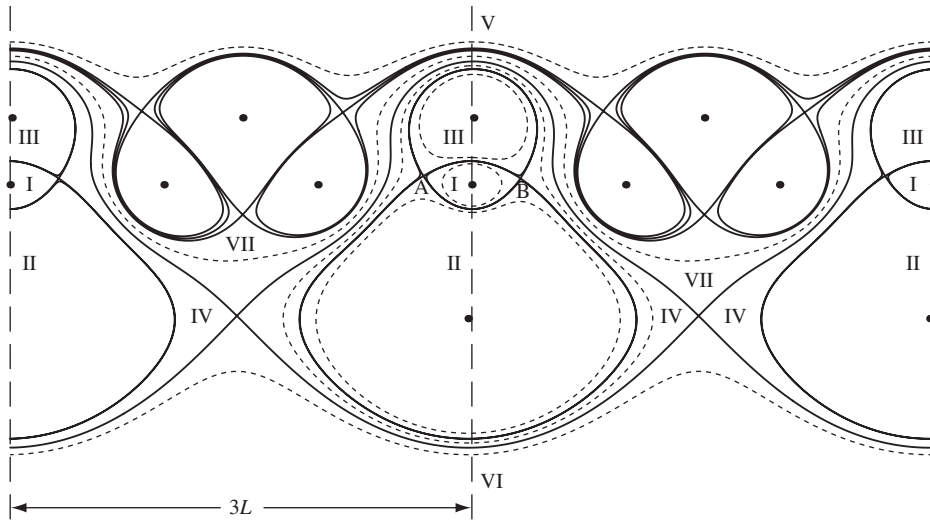
Fig. 4. Phase plane for the three-vortex system with strengths $(2, 1, -3)$ in a periodic strip. The value of $\Xi \approx L(0.024 + i0.870)$ has been determined such that the relative equilibrium corresponding to point A will translate in the periodic direction (along the x-axis of coordinates). Solid lines are again separatrices delimiting the various domains of motion. Dashed lines correspond to real space motions shown in Fig. 5. Note the similarity between the central part of this figure and the phase plane diagram in Fig. 1.
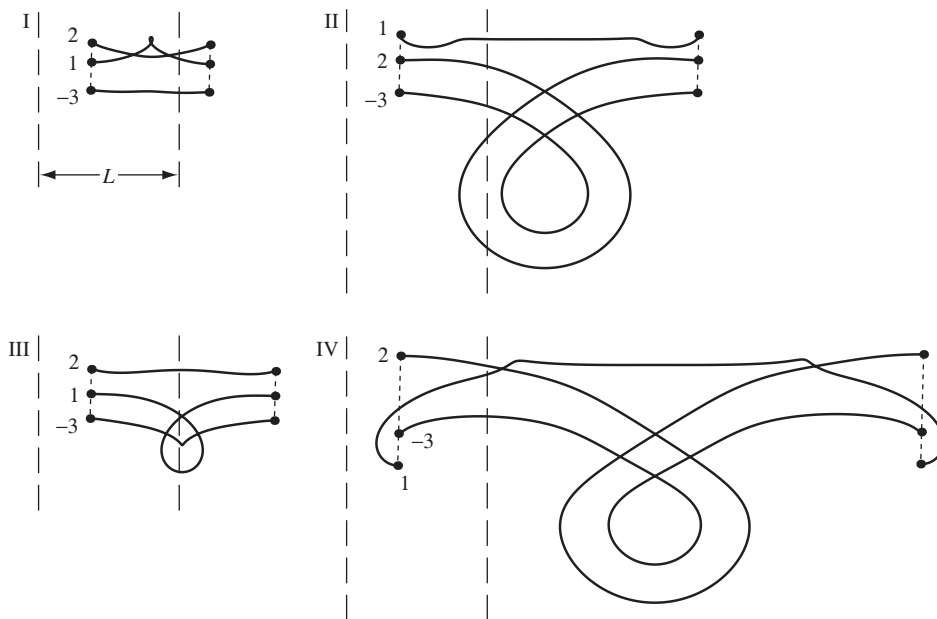

Fig. 5. Physical plane trajectories of three vortices in a periodic strip. The trajectories correspond to the dashed lines in domains I–IV in Fig. 4. These trajectories may be compared to the trajectories shown in Fig. 1.

strengths 1 and -3. This feature of up- and downstream migration of one or more of the vortices is true for all regions that exit and re-enter the periodic boundaries in the phase plane. In Fig. 6(VII), corresponding to one of the thin, winding domains in Fig. 4, we have quite complicated vortex trajectories with loops and cusps and considerable motion of individual vortices in the periodic direction. A vortex may move many periods L during one period of the relative motion, as one might have anticipated from the phase plane being a wider strip than the physical strip of the original problem.
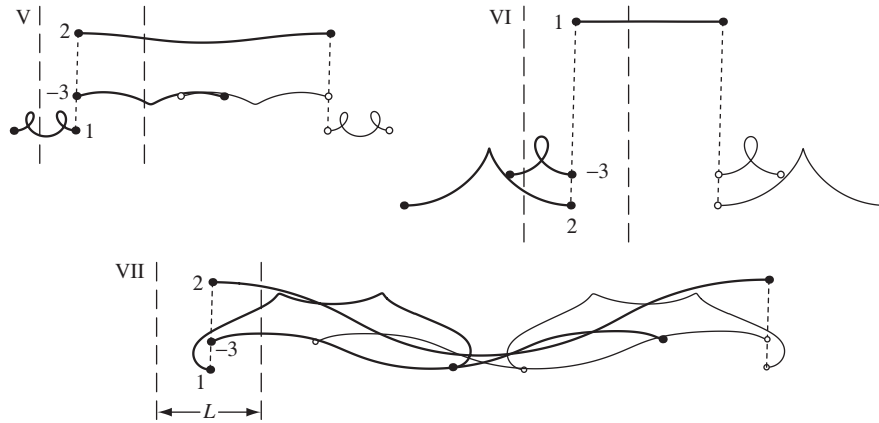
Fig. 6. Additional physical space trajectories corresponding to the phase plane in Fig. 4, where the corresponding phase space curves are shown as dashed lines in the respective domains.

There is a tendency to dismiss unstable equilibria as not being relevant to the dynamics. We argue that this view is too restrictive. Even though the relative equilibria are unstable, in some cases (such as Fig. 4) *all* finite amplitude perturbations can lead to a re-appearance of these states (or states close to them) consisting of the same three vortices after a relatively short time. The slowing down of the dynamics that occurs in the vicinity of any equilibrium then guarantees that these configurations will show up as long-lived transients in the dynamics.

Just as was the case on the infinite plane, we note that the system of advecting vortices is itself a solution to the equations of periodic rows of point vortices. Thus, in Fig. 4 the six advecting vortices (per period) form a stationary configuration. The argument is the same as for the infinite plane case.

4. "Exotic wakes" with three vortices shed per cycle

We now want to apply the solution of the three-vortex problem in the periodic strip to the problem of vortex wakes in the same spirit that the two-vortices-in-a-strip solution has been applied to the Kármán vortex street and its variants for decades.

First, we show in Fig. 7 what may be the most 'stable'—and, hence, reproducible—three-vortices-per-period wake pattern known. This pattern has been seen experimentally and in several numerical simulations using considerably different methods. We show an experimental streakline picture due to Williamson (private communication) and a gray scale vorticity plot from a recent simulation using a novel numerical method by Ponta and Aref (2006). The Reynolds number, frequency and amplitude of oscillation of the cylinder are closely matched between experiment and simulation.

If we view this state from the vantage point of the three-vortices-in-a-strip solution just reviewed, we see that the two vortices on the lower side of the wake are moving more rapidly downstream than the single vortex on the upper side. This is the kind of motion associated with domains V and VI in Fig. 4 (see also Fig. 6). While one might see motions in the data of the somewhat "tame" variety in Fig. 5, the more "wild" trajectories consisting of long-range excursions with loops and twists as in Fig. 6 (e.g., panel VII) do not seem to have been observed. Thus, the first general conclusion is that the richness of a phase diagram such as Fig. 4 has not been captured in the current experimental or numerical data.

The analog of the Kármán vortex street configurations for three vortices per strip are the relative equilibria that occur and that are manifested as intersections of the separatrices shown in Fig. 4. Several such intersections are clearly visible. All of them are saddle points so we know a priori that the corresponding three-vortex configurations are unstable. Stremler (2003) has shown that the analytical characterization of these states is both possible and relatively simple. We give a different approach to these results here.

Set $c_1 = \cot[\pi(z_2 - z_3)/L]$, $c_2 = \cot[\pi(z_3 - z_1)/L]$ and $c_3 = \cot[\pi(z_1 - z_2)/L]$. From the addition formula for the cotangent function c_1, c_2 and c_3 are related by

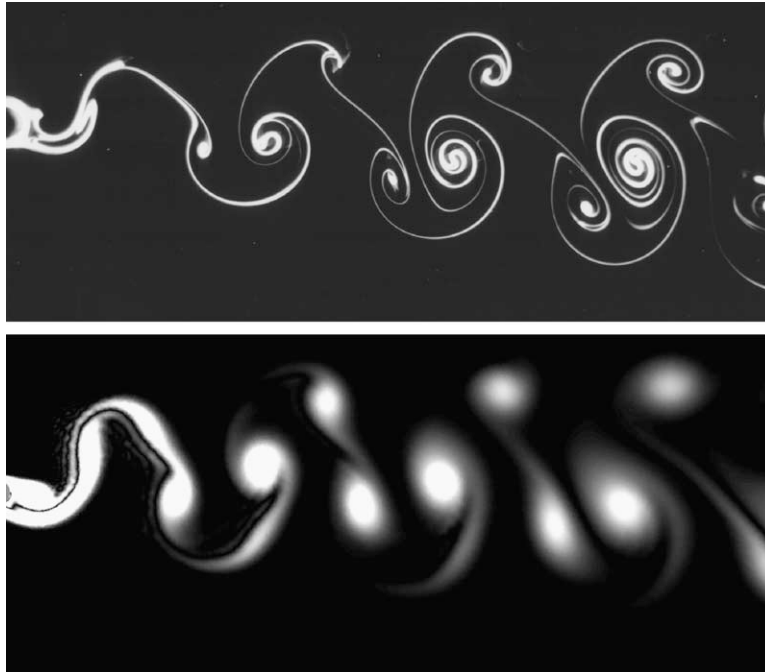$$c_1 c_2 + c_2 c_3 + c_3 c_1 = 1. \tag{16}$$

Fig. 7. Top: flow visualization of P + S wake pattern behind an oscillating cylinder at Re = 140 (C.H.K. Williamson, private communication). Bottom: gray scale plot of the vorticity field from a numerical simulation by Ponta and Aref (2006).
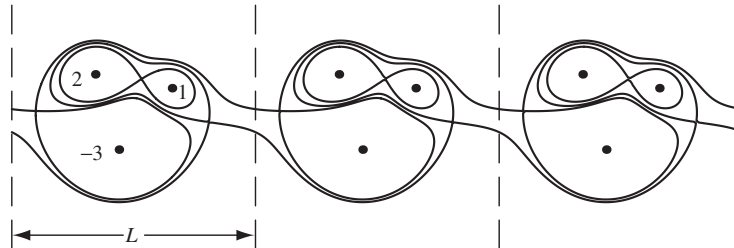

Fig. 8. Streamlines in the co-moving frame for "vortex streets" with three vortices per period. This configuration, which corresponds to point A in Fig. 4, translates along the periodic direction.

With this notation, Eqs. (12)–(14), with the velocities on the left-hand sides set to the common translation velocity of the pattern, $U - iV$, become

$$2L(V + iU) = \Gamma_2 c_3 - \Gamma_3 c_2 = \Gamma_3 c_1 - \Gamma_1 c_3 = \Gamma_1 c_2 - \Gamma_2 c_1. \tag{17}$$

Taking the difference between any two of Eqs. (17), and using that the vortex strengths sum to zero, gives

$$c_1 + c_2 + c_3 = 0. \tag{18}$$

Now, view Eqs. (16)–(18) and $\Gamma_1 + \Gamma_2 + \Gamma_3 = 0$ as relations between components of "vectors" $\mathbf{e} = (1, 1, 1)$, $\boldsymbol{\Gamma} = (\Gamma_1, \Gamma_2, \Gamma_3)$ and $\mathbf{c} = (c_1, c_2, c_3)$ in a three-dimensional complex vector-space. Let the dot and cross product continue to be calculated as they would be for vectors with real components. The vanishing of the sum of the circulations would then tell us that $\mathbf{e} \cdot \boldsymbol{\Gamma} = \Gamma_1 + \Gamma_2 + \Gamma_3 = 0$. Similarly, Eq. (18) tells us that $\mathbf{e} \cdot \mathbf{c} = 0$. Finally, Eq. (17) may be written in terms of the vectors $\boldsymbol{\Gamma}$ and $\mathbf{c}$ as

$$\boldsymbol{\Gamma} \times \mathbf{c} = 2L(V + iU)\mathbf{e}. \tag{19}$$

Since the vector-space is three-dimensional, the vectors $\mathbf{e}$, $\boldsymbol{\Gamma}$ and $\mathbf{e} \times \boldsymbol{\Gamma}$ form an orthogonal basis. Any vector, in particular $\mathbf{c}$, may be expanded in terms of this basis. Thus, we have

$$\mathbf{c} = \lambda \mathbf{e} + \mu \boldsymbol{\Gamma} + v \mathbf{e} \times \boldsymbol{\Gamma}, \tag{20}$$

where λ, μ and v are to be determined.

From $\mathbf{e} \cdot \mathbf{c} = 0$ we immediately get $\lambda = 0$. We then see from (20) that

$$\boldsymbol{\Gamma} \times \mathbf{c} = v \boldsymbol{\Gamma} \times (\mathbf{e} \times \boldsymbol{\Gamma}) = v(\boldsymbol{\Gamma} \cdot \boldsymbol{\Gamma})\mathbf{e}, \tag{21}$$

where $\boldsymbol{\Gamma} \cdot \boldsymbol{\Gamma} = \Gamma_1^2 + \Gamma_2^2 + \Gamma_3^2 = -2(\Gamma_1\Gamma_2 + \Gamma_2\Gamma_3 + \Gamma_3\Gamma_1) = -2\sigma_2$, with σ_2 the second symmetric function of the Γ's.

From the relations (16) and (18) we have $\mathbf{c} \cdot \mathbf{c} = -2$. Thus from (20) with $\lambda = 0$,

$$-2 = \mathbf{c} \cdot \mathbf{c} = (\mu^2 + v^2\mathbf{e} \cdot \mathbf{e})\boldsymbol{\Gamma} \cdot \boldsymbol{\Gamma} = -2\sigma_2(\mu^2 + 3v^2) \quad \text{or} \quad \sigma_2(\mu^2 + 3v^2) = 1. \tag{22}$$

Comparison of (19) and (21) gives

$$v = -\frac{L(V + \mathrm{i}U)}{\sigma_2}, \quad \mu^2 = \frac{\sigma_2 - 3L^2(V + \mathrm{i}U)^2}{\sigma_2^2}. \tag{23}$$

Using these values now gives the values of c_1, c_2 and c_3 that correspond to a given velocity of translation, solving in essence the same problem for "vortex streets" with three vortices per period that Eq. (6) solves for the usual two-vortices-per-strip problem. In particular, for a configuration that translates in the periodic direction, we want $V = 0$. Then (23) says that v is pure imaginary. For the examples considered here, these formulae were used to determine relative equilibrium configurations that translate in the periodic direction. The value of Ξ is then determined from the positions of the vortices. This connection is nonlinear, since the condition for translation in the periodic direction gives values of c_1, c_2 and c_3, whereas Ξ is linear in the vortex positions themselves. We have not found an analytic resolution to this at present, and so have solved for the positions numerically.

In Fig. 8 we show the dividing streamlines in a frame of reference moving with the vortices for the configuration that corresponds to the saddle point labelled A in Fig. 4. This state translates in the periodic direction and the streamline pattern in Fig. 8 may be compared to that in Fig. 3. We are not aware of experiments or numerical simulations that have seen patterns such as these emerge during vortex shedding.

4.1. Stationary wake patterns

We conclude this section by returning to the observation that the configuration of advecting vortices in phase space, considered as capable of dynamic motion, is a relative equilibrium of the three rows of vortices that it represents. We have a parametrization for these solutions as follows: choose any three real numbers, γ_1, γ_2, γ_3, all nonzero but that sum to zero. There is no restriction in assuming $\gamma_1 \geqslant \gamma_2 > 0$ and $\gamma_3 < 0$. Place a row of vortices of circulation γ_3^{-1} at nL, $n = 0, \pm1, \pm2, \ldots$. Place a second row of vortices of circulation γ_2^{-1} at $(-\Xi + nL\gamma_3)/\gamma_2$, where Ξ is an arbitrary complex number different from 0, and, again, $n = 0, \pm1, \pm2, \ldots$. Finally, place a third row of vortices of circulation γ_1^{-1} at $(\Xi + nL\gamma_3)/\gamma_1$, $n = 0, \pm1, \pm2, \ldots$. From our previous developments, these three rows of vortices will constitute a relative equilibrium. In fact, it will be a stationary equilibrium since, as we saw in Section 2, an equilibrium can only translate if the sum of the strengths of the point vortices vanishes, and with the stipulations on γ_1, γ_2, γ_3, we have $\gamma_1^{-1} + \gamma_2^{-1} + \gamma_3^{-1} > 0$. These configurations are parametrized by γ_1/γ_2 (or any other ratio of the three originally chosen numbers) and by the real and imaginary part of Ξ. That is, we have a three-parameter family of solutions.

As already indicated, if γ_1/γ_2 (or any other ratio of the three originally chosen numbers) is rational, this configuration has a period that is a multiple of L. If γ_1/γ_2 is irrational, the configuration does not have long-range order in the direction of the parallel rows.

Since these configurations are stationary, i.e., their self-induced velocity of translation vanishes, we suggest that they may arise as models of "exotic" momentumless wakes.

In addition to these vortex wake patterns, the approach of Stremler (2003) allows one to search for stationary patterns with three vortices per period and net circulation zero. We showed earlier for general N that a relative equilibrium of vortices can only translate if the sum of the vortex strengths vanishes. This does not mean, of course, that such a pattern must always translate. Indeed, stationary equilibria are possible but, as it turns out, only if all the vortices are on a line.

5. Conclusions, discussion and outlook

First, we comment on the very limited control one has to ''set'' the vorticity distribution in experiments or full numerical simulations of vortex wakes shed by bluff bodies. In the type of theory we have pursued here we think of the vortex positions and strengths as independent variables that can be arranged at will. In an experiment, whether in the lab or on the computer, the configuration of vortices that makes up the wake is, of course, ''set'' by the shedding process at the bluff body. In experimental work we have the freedom to oscillate the body, streamwise or transversally, to rotate the body, to deploy various body shapes, and to consider multiple wake-producing bodies. However, the control of what kind of vortex wake pattern one produces is always indirect. Secondary processes take place in the near wake, even after the primary shedding, before the vortices arrange themselves into the final vortex-street pattern. The final configuration results from combinations of vortex splitting and merging events that have been observed in both experiments and numerical simulations. These processes in the near-wake region essentially alter the number, position and individual strengths of the vortex structures available to form the vortex street (or whatever pattern ultimately emerges). Although these processes show a dependence on the kinematics of the body motion [and indeed may be triggered by changes in the trajectory parameters as shown by Ponta and Aref (2006)], we have only limited understanding of how to effect vortex wake ''control'' by manipulation of the body kinematics. The ''phase diagram'' of Williamson and Roshko (1988) is probably the closest answer that we have today for addressing such issues. We have recently tried to rationalize the level curves in this diagram based on dynamical arguments in Ponta and Aref (2005).

From the standpoint of theory this may mean that the main reason we have not observed the full richness of a diagram such as Fig. 4 is simply that the configurations accessible through the above-mentioned controls of vortex shedding do not allow a full exploration of this space. These remarks suggest that a more global view of vortex wakes be taken, including wakes behind heaving and pitching airfoils, behind bodies that are started and/or stopped impulsively, behind fences and steps, behind arrays of bodies, etc., and that one not narrow the field to the study of wakes behind circular cylinders whether stationary or in harmonic oscillation.

Second, the representation of what are in reality distributed vortices in a viscous fluid by point vortices in an ideal fluid is always a matter of concern. This is true even for the usual Kármán street where the real vortices are subject to viscous dispersion and decay as they propagate downstream, yet the model operates with infinite rows of time-invariant, identical vortices. This issue has occupied many researchers over time. The best one can say is that, although the individual vortices do re-adjust and decay somewhat as they move downstream, the circulation around each individual vortex is preserved for a surprisingly long time, and so the far field of the vortices, which is what its neighbors see to first order, is accurately given by the point vortex model for longer than one might assume. These statements are based on numerical simulation data by Ponta and Aref that we hope to publish soon.

We should add to this that when we see loops and cusps in the trajectories of point vortices modelling wake vortices, the finite area vortices that make up real vortex wakes would not be expected to execute nearly as dramatic excursions. A small loop or cusp in a point vortex trajectory could correspond to a much gentler and less noticeable ''nutation'' of a finite area vortex, i.e., a precession of the structure coupled to some internal re-arrangement of the vorticity distribution.

Finally, Kármán's ultimate objective with his vortex wake model was to establish a formula for the drag on the bluff body producing the wake. In this he succeeded with what we today know as the *Kármán drag law*. The vortex-street patterns with three vortices per period, e.g., those illustrated in Fig. 8, should also yield a drag law much like von Kármán's. However, it may be possible to extend this further and derive a drag law even for cases where the three-vortex-per-cycle wake is evolving downstream. We leave this as an open problem to which we intend to return.

References

Aref, H., 1983. Integrable, chaotic and turbulent vortex motion in two-dimensional flows. Annual Review of Fluid Mechanics 15, 345–389.

Aref, H., 1989. Three-vortex motion with zero total circulation: addendum. Journal of Applied Mathematics and Physics (ZAMP) 40, 495–500.

Aref, H., Stremler, M.A., 1996. On the motion of three point vortices in a periodic strip. Journal of Fluid Mechanics 314, 1–25.

Birkhoff, G., Fisher, J., 1959. Do vortex sheets roll up? Rendiconti del Circolo matematico di Palermo 8, 77–90.

Dolaptschiew, B., 1938. Störungsbewegungen (Bahnen) der einzelnen Wirbel der Kármánschen Wirbelstrasse. Zeitschrift für Angewandte Mathematik und Mechanik (ZAMM) 18, 263–271.

Domm, U., 1956. Über die Wirbelstrassen von geringster Instabilität. Zeitschrift für Angewandte Mathematik und Mechanik (ZAMM) 36, 367–371.

Friedmann, A., Poloubarinova, P., 1928. Über fortschreitende Singularitäten der ebenen Bewegung einer inkompressiblen Flüssigkeit. Recueil de Géophysique, Tome V, Fascicule II, Leningrad, pp. 9–23 (Russian with German summary).

Kochin, N., 1939. On the instability of von Kármán's vortex streets. Doklady Acadademii Nauk SSSR 24, 19–23.

Lamb, H., 1932. Hydrodynamics, sixth ed. Cambridge University Press, Cambridge.

Maue, A.W., 1940. Zur Stabilität der Kármán schen Wirbelstrasse. Zeitschrift für Angewandte Mathematik und Mechanik (ZAMM) 20, 129–137.

Newton, P.K., 2001. The *N*-Vortex Problem—Analytical Techniques. Applied Mathematical Sciences, vol. 145. Springer, New York.

Ponta, F.L., Aref, H., 2005. Vortex synchronization regions in shedding from an oscillating cylinder. Physics of Fluids 17, 011703.

Ponta, F.L., Aref, H., 2006. Numerical experiments on vortex shedding from an oscillating cylinder. Journal of Fluids and Structures 22, 327–344.

Rosenhead, L., 1929. Double rows of vortices with arbitrary stagger. Proceedings of the Cambridge Philosophical Society 25, 132–138.

Rosenhead, L., 1931. The formation of vortices from a surface of discontinuity. Proceedings of the Royal Society, London, Series A 134, 170–192.

Rott, N., 1989. Three-vortex motion with zero total circulation. Journal of Applied Mathematics and Physics (ZAMP) 40, 473–494 [With an Addendum by H. Aref (1989)].

Stremler, M.A., 2003. Relative equilibria of singly periodic point vortex arrays. Physics of Fluids 15, 3767–3775.

Williamson, C.H.K., Roshko, A., 1988. Vortex formation in the wake of an oscillating cylinder. Journal of Fluids and Structures 2, 355–381.